

Effect of synthesis route on the hydrogen storage properties of $2\text{MgH}_2\text{-Fe}$ compound doped with LiBH_4 .

Author: C. Gosselin^{*}, S. Deledda[†], B.C. Hauback[†], J. Huot^{*}

^{*}Hydrogen Research Institute, Université du Québec à Trois-Rivières, 3351 des Forges, Trois-Rivières, Québec G9A 5H7, Canada

[†] Institute for Energy Technology, Department of Physics, P.O. Box 40, NO-2027 Kjeller, Norway

ABSTRACT

The hydrogen storage properties of a 2:1 mole ratio of MgH_2 and Fe with or without 10 wt. % of LiBH_4 were investigated. Two doping methods were used: the first one consisted of two steps: first the $2\text{MgH}_2\text{+Fe}$ mixture was ball milled for 10 hours and subsequently LiBH_4 was added and milling resumed for 1 more hour. In the second method all materials were mixed and ball milled for 10 hours. The first method produced materials with an hydrogen dehydrogenation capacity of 2,69 wt.% at 623 K and that could re-absorb 2,93 wt.% H_2 . The materials made by the second method presented a hydrogen dehydrogenation capacity of 2,98 wt.% at 623 K and re-absorbed 3,10 wt.% H_2 . For both methods, the rehydrided sample consisted only of MgH_2 . The reversibility of the reaction was enhanced with the LiBH_4 , but this additive, by acting as a catalyst for the formation of MgH_2 , precludes the formation of Mg_2FeH_6 .

KEYWORDS

Metal hydrides, hydrogen absorbing materials, lithium borohydride, kinetics

INTRODUCTION

Because of their high hydrogen storage capacities, magnesium-based alloys have been actively considered for hydrogen storage applications [1]. However, the high temperature of operation and relatively slow kinetics drastically reduce the practicality of using this type of materials. Instead of using these alloys for hydrogen storage an elegant solution is to use them for thermal storage [2, 3]. The ternary alloy Mg_2FeH_6 has been discovered by Didisheim et al who synthesized it at 450°C under high hydrogen pressure (20-120 bar) [4]. This hydride store 5.5 wt.% of hydrogen compare to 7.6 wt.% for MgH_2 . However, Mg_2FeH_6 could be more suitable for heat storage applications because of its lower hydrogen dissociation pressure (66 bar compared to 104 bar at 500°C)[5]. This means that the heat storage tank could be operated at lower pressure and thus reducing cost.

The beneficial effect of LiBH_4 on hydrogen sorption kinetic of MgH_2 has been well established [6, 7]. Puskiel and Gennari have shown that the composite powder Mg_{15}Fe doped with ~ 10 mol.% LiBH_4 shows much higher capacity and faster kinetics than the undoped composite [8]. Deng et al used Mg_2FeH_6 as a catalyst for LiBH_4 and found that the sorption properties of LiBH_4

are improved [9]. In a recent investigation, Li et al showed that in the mixtures $x\text{LiBH}_4 + (1-x)\text{Mg}_2\text{FeH}_6$ ($x < 0.5$) both hydrides simultaneously release hydrogen [10].

We report here the use of LiBH_4 as a catalyst for hydrogen sorption of Mg_2FeH_6 . Two different synthesis pathways were studied. In one MgH_2 and Fe were first milled together and LiBH_4 was added for the last hour of milling. In the other method all raw materials were mixed and milled together. In this way we could test the impact of synthesis route on the final structure and hydrogen storage properties of the material.

EXPERIMENTAL

Commercial LiBH_4 (95%), MgH_2 (98%) and Fe (99,9%) powders were all purchased from Alfa Aesar and used without further purification. Ball milling was performed under argon using a SPEX 8000 mill. Stoichiometric amount of 2MgH_2 and Fe for a total of 3g were placed in a stainless steel crucible with 4 stainless steel balls to obtain ball to powder weight ratio of 10:1. To prevent oxidation all samples were stored and handled in an argon filled glove box.

Three different composites were synthesized. For the first one, (compound A) 2MgH_2 and Fe powders were ball milled for ten hours. The second sample (compound B) 2MgH_2 and Fe powders were first milled ten hours and thereafter 10 wt.% of LiBH_4 was added and milling resumed for one more hour. The third sample (compound C) 2MgH_2 , Fe and 10 wt.% of LiBH_4 were mixed together and milled for ten hours.

Crystal structure was analyzed from X-ray powder diffraction patterns registered on a Bruker D8 Focus apparatus with $\text{CuK}\alpha$ radiation. To prevent reaction between sample and air during the data collection an argon-sealed sample holder was used. This sample holder is responsible for the broad amorphous-like peak below 35 degrees. Rietveld refinements were performed using the Topas software via the fundamental parameter approach [11].

The hydrogen sorption properties of the samples were measured with a homemade Sievert-type apparatus. The dehydrogenations were made at 623 K under a pressure of 0,1 MPa. Samples were thereafter exposed to a hydrogen pressure of 3 MPa at 623 K for hydrogenation.

RESULTS AND DISCUSSION

Figure 1 shows the X-ray powder diffraction of all samples after synthesis. Phase's abundances as determined from Rietveld refinement are shown in Table 1. The slight shift of the main iron peak in pattern C compare to the other two patterns is due to zero offset. It is clear that the amount of Fe derived from these analyses is too large. For instance, if the iron in Mg_2FeH_6 is taken into account then the total amount of iron is about 65wt.% which is higher than the nominal stoichiometry (about 55 wt.%). The reason for such a discrepancy is likely due to the uncertainties caused by the strong fluorescence of iron caused by the incident $\text{Cu K}\alpha$ radiation. . Another possible explanation is that the discrepancy is due to micro-absorption and an

underestimation of the Mg-containing phases. It has been shown that Mg_2FeH_6 is usually capped by iron [12]. Since the attenuation of Cu radiation in Fe is considerably larger than in magnesium, we expect that micro-absorption in iron will ‘mask’ all Mg-based phases, which in turn will be underestimated during the Rietveld refinement. Therefore, numbers given in Table 1 should only be taken as a reference. We report them here in order to have a quantitative comparison between the phase abundance of MgH_2 and Mg_2FeH_6 .

Figure 1

Table 1. Phase abundances in wt.% of as-milled samples as determined from Rietveld refinement. Uncertainty on each value is ± 1 .

Sample	Fe	MgH_2	Mg_2FeH_6
Nominal $2\text{MgH}_2 + \text{Fe}$	49	51	---
Nominal $2\text{MgH}_2 + \text{Fe} + 10 \text{ wt.}\% \text{LiBH}_4$	44	46	
$2\text{MgH}_2 + \text{Fe}$ ball milled 10 hours	50	23	27
$2\text{MgH}_2 + \text{Fe}$ ball milled 10 hours + 10 wt.% LiBH_4 ball milled 1 more hour	52	22	26
$2\text{MgH}_2 + \text{Fe} + 10 \text{ wt.}\% \text{LiBH}_4$ ball milled 10 hours	64	36	--

It is clear from the phases abundances reported in Table 1 that adding LiBH_4 after 10 hours of milling and continue milling for one more hour does not have any impact on the phase composition. However, milling the mixture $2\text{MgH}_2 + \text{Fe} + 10 \text{ wt.}\% \text{LiBH}_4$ totally suppress the formation of Mg_2FeH_6 .

The values of crystallites size are given in Table 2. It confirms that adding LiBH_4 after 10 hours have minimal impact on the crystal structure of the material: the crystallites size is only slightly increased. On the other hand, adding LiBH_4 at the beginning of milling produces bigger crystallite sizes.

Table 2. Crystallites size in nm of different phases in as-milled samples as determined from Rietveld refinement. Uncertainty on last significant digit each value is given in parenthesis.

Sample	Fe	MgH_2	Mg_2FeH_6
$2\text{MgH}_2 + \text{Fe}$ milled 10 hours	14.4(3)	5.7(8)	8.6(5)
$2\text{MgH}_2 + \text{Fe}$ milled 10 hours + 10 wt.% LiBH_4 and milled 1 more hour	15.3(2)	6.1(7)	9.6(5)
$2\text{MgH}_2 + \text{Fe} + 10 \text{ wt.}\% \text{LiBH}_4$ milled 10 hours	24.6(5)	8.3(7)	--

Hydrogen sorption

After milling, the samples were first desorbed at 623 K under an initial pressure of 0.1 MPa. The dehydrogenation curves are shown in Figure 2a. It is clear that these samples have different

kinetics and capacities. As ball milling was performed under argon, the nominal capacity should be 3.8 wt.%, not taking into account LiBH_4 . We see that the only sample having a capacity close to the nominal one is the undoped sample. Doping has the effect of reducing the capacity and dehydrogenation kinetic.

Figure 2

The first hydrogenation kinetics are shown in figure 2b. Here the trend is reversed: the undoped sample has a lower capacity than the doped ones. Kinetics are quite fast but the capacities are far from the nominal value (5.6 wt.% assuming full hydrogenation to Mg_2FeH_6). Such variation of capacities between the first dehydrogenation and hydrogenation is somewhat expected because the amount of hydrogen available during milling is not sufficient to totally synthesize Mg_2FeH_6 as there are only 4 H in the original composition. Thus, if the microstructure is optimal and if LiBH_4 really catalyze the reaction we expect to have higher capacities in subsequent cycles. For this reason, we performed 3 more cycles for each sample.

Figure 3 shows three consecutive hydrogenation/dehydrogenation cycles for the undoped sample (sample A). We see a slight decrease in capacity at each hydrogenation cycle. The first dehydrogenation capacity is higher than the first hydrogenation. This is probably due to a remnant of hydrogen in the sample. But the subsequent dehydrogenation capacity is the same as hydrogenation. Thus, we could conclude that the undoped sample slowly loses capacity upon cycling and that the total capacity is much less than what is expected for a full reaction.

Figure 3

Cycling of sample B is shown in Figure 4. There is a slight decrease of capacity between the first and second dehydrogenation but all hydrogenation saturates at the same value. The hydrogenation capacity is slightly higher (about 0.1 wt.%) than the dehydrogenation capacity but this is due to systematic error of the apparatus caused by the very fast hydrogenation kinetic. The main result here is that doping with LiBH_4 seems to be beneficial for cycling properties.

Figure 4

Cycling of sample C is presented in Figure 5. Here, the loss of capacity between the first and second dehydrogenation is very small and the hydrogenation capacities are the same. However, dehydrogenation kinetic is slower than for sample B. Thus, having a better mixing of LiBH_4 in $2\text{MgH}_2 + \text{Fe}$ mixture slightly improves cycling but has a detrimental effect on the dehydrogenation kinetics.

Figure 5

For all samples the hydrogen capacity was much smaller than the expected capacity if a complete reaction took place. To verify what kind of hydrogenation reaction occurred we took

a powder diffraction pattern of each sample after the third hydrogenation. These patterns are shown in Figure 6.

Figure 6

We see that for all samples only MgH_2 is formed upon hydrogenation and there is no evidence of formation of Mg_2FeH_6 . Those results seem to confirm that the presence of $LiBH_4$ inhibits the formation of Mg_2FeH_6 , as observed in the sample C after milling. Crystallite sizes as determined from Rietveld refinement are shown in Table 3. Comparing with the as-milled values reported in Table 2 it is clear that an important grain growth occurred for the MgH_2 phase. However this grain growth was not the same for all samples. Even if the MgH_2 phase in the undoped sample experienced a ten-fold increase, its crystallite size is still less than both doped samples. On the other hand, the iron phase showed an increase of crystallite size in the undoped sample but a decrease in the doped samples. This may be due to some interaction of Fe with $LiBH_4$ but the real explanation is still unclear.

Table 3. Crystallites size in nm of different phases in samples after 3 hydrogen dehydrogenation/hydrogenation cycles as determined from Rietveld refinement. Uncertainty on last significant digit each value is given in parenthesis.

Sample	Fe	MgH_2
$2MgH_2 + Fe$ milled 10 hours	41(1)	53(6)
$2MgH_2 + Fe$ milled 10 hours + 10 wt.% $LiBH_4$ and milled 1 more hour	7.4(4)	80(7)
$2MgH_2+Fe + 10$ wt.% $LiBH_4$ milled 10 hours	17(1)	167(21)

The results presented in this work may seem contradictory to the one of Li et al who showed that $LiBH_4$ and Mg_2FeH_6 release hydrogen simultaneously and that in fact $LiBH_4$ may be embedded in Mg_2FeH_6 forming a $Li_xMg_{2-2x}(BH_4)_x(FeH_6)_{1-x}$ structure [10]. However, the composites produced by Li et al were synthesized following a different procedure: Mg_2FeH_6 was first synthesized by ball milling, subsequently sintered under hydrogen and thereafter milled with $LiBH_4$. In our case there was no sintering intermediate step and in all of our samples the amount of MgH_2 was non negligible. It can be thus be inferred that the H-sorption properties of this system are strongly dependent on the synthesis route and initial composition of the composite powders. Therefore, comparison of hydrogen sorption properties of Mg_2FeH_6 prepared by different authors and methods should be made with great caution.

CONCLUSION

In this study we showed that $LiBH_4$ instead of acting like a catalyst for the synthesis of Mg_2FeH_6 in fact preclude its formation by catalyzing the formation of MgH_2 . This conclusion may seem contradictory with previous works where a complex hydride with both double-cation and double-anion was possibly formed [10]. However, in the present investigation the ratio of $LiBH_4$ and Mg_2FeH_6 is much different. In our case the stoichiometry is $0.5 LiBH_4 + Mg_2FeH_6$ while in

the work of Li et al the stoichiometry is $0.5 \text{ LiBH}_4 + 0.5 \text{ Mg}_2\text{FeH}_6$. Also, milling process could be energetically quite different.

In the case of Deng et al their stoichiometry is $5 \text{ LiBH}_4 + \text{Mg}_2\text{FeH}_6$ which effectively it is a situation where Mg_2FeH_6 is the additive to LiBH_4 [9]. Therefore, they treated Mg_2FeH_6 as a catalyst for LiBH_4 and as their amount of LiBH_4 is 10 times higher than in the present study comparing our results with theirs is problematic.

Puszkiel and Gennari studied the composite powder Mg_{15}Fe doped with 10% LiBH_4 [8]. In this system the details of synthesis play a crucial role in the final crystal structure, microstructure and H-sorption properties.

Acknowledgements

C. Gosselin would like to thank Hydro-Québec for a summer fellowship. J. Huot thanks the Research Council of Norway for funding that permitted a sabbatical leave at the Institute for Energy Technology (IFE) in Norway.

Figures caption

Figure 1: X-ray diffraction patterns for: A- $2\text{MgH}_2+\text{Fe}$ ball milled 10 hours; B- $2\text{MgH}_2+\text{Fe}$ ball milled for 10 hours and further milled with LiBH_4 for 1 more hour; C- $2\text{MgH}_2+\text{Fe}$ and LiBH_4 ball milled for 10 hours.

Figure 2. Sorption kinetics at 623 K of a) first dehydrogenation under initial pressure of 0,1 Mpa, b) first hydrogenation under 3 Mpa. The single curves refer to: A- $2\text{MgH}_2+\text{Fe}$ ball milled 10 hours; B- $2\text{MgH}_2+\text{Fe}$ ball milled for 10 hours and further milled with LiBH_4 for 1 more hour; C- $2\text{MgH}_2+\text{Fe} + \text{LiBH}_4$ ball milled for 10 hours.

Figure 3: Three cycles of dehydrogenation-hydrogenation of the composite $2 \text{MgH}_2\text{-Fe}$ ball milled 10 hours

Figure 4: Three cycles of dehydrogenation-hydrogenation of $2\text{MgH}_2+\text{Fe}$ ball milled 10 hours, and further milled with LiBH_4 for 1 more hour.

Figure 5: Three cycles of dehydrogenation-hydrogenation of $2\text{MgH}_2+\text{Fe}$ and LiBH_4 ball milled 10 hours.

Figure 6: X-ray diffraction patterns after 3 dehydrogenation/hydrogenation cycles. A- $2\text{MgH}_2+\text{Fe}$ milled 10 hours; B- $2\text{MgH}_2+\text{Fe}$ milled for 10 hours + 5wt.% LiBH_4 and milled for 1 more hour; C- $2\text{MgH}_2+\text{Fe} + 5\text{wt.}\% \text{LiBH}_4$ milled for 10 hours.

References

- [1] B. Sakintuna, F. Lamari-Darkrim, M. Hirscher, Metal hydride materials for solid hydrogen storage: A review, *International Journal of Hydrogen Energy*, 32 (2007) 1121-1140.
- [2] D.N. Harries, M. Paskevicius, D.A. Sheppard, T.E.C. Price, C.E. Buckley, Concentrating Solar Thermal Heat Storage Using Metal Hydrides, *Proceedings of the IEEE*, 100 (2012) 539-549.
- [3] B. Bogdanovic, B. Spliethoff, A. Ritter, The Magnesium Hydride System for Heat Storage and Cooling, *Zeitschrift für Physikalische Chemie Neue Folge*, 164 (1989) 1497-1508.
- [4] J.-J. Didisheim, P. Zolliker, K. Yvon, P. Fisher, J. Schefer, M. Gubelmann, A.F. Williams, Dimagnesium iron(II) hydrides, Mg_2FeH_6 , containing Octahedral FeH_6^{4-} anions, *Inorg. Chem.*, 23 (1984) 1953-1957.
- [5] B. Bogdanovic, A. Reiser, K. Schlichte, B. Spliethoff, B. Tesche, Thermodynamics and dynamics of the Mg-Fe-H system and its potential for thermochemical thermal energy storage, *Journal of Alloys and Compounds*, 345 (2002) 77-89.
- [6] J.F. Mao, Z. Wu, T.J. Chen, B.C. Weng, N.X. Xu, T.S. Huang, Z.P. Guo, H.K. Liu, D.M. Grant, G.S. Walker, X.B. Yu, Improved Hydrogen Storage of $LiBH_4$ Catalyzed Magnesium, *J. Phys. Chem. C*, 111 (2007) 12495-12498.
- [7] S.R. Johnson, P.A. Anderson, P.P. Edwards, I. Gameson, J.W. Prendergast, M. Al-Mamouri, D. Book, I.R. Harris, J.D. Speight, A. Walton, Chemical activation of MgH_2 : a new route to superior hydrogen storage materials, *Chem. Commun.*, 2005 (2005) 2823-2825.
- [8] J.A. Puzkiel, F.C. Gennari, Reversible hydrogen storage in metal-doped Mg- $LiBH_4$ composites, *Scripta Materialia*, 60 (2009) 667-670.
- [9] S.S. Deng, X.Z. Xiao, L.Y. Han, Y. Li, S.Q. Li, H.W. Ge, Q.D. Wang, L.X. Chen, Hydrogen storage performance of $5LiBH_4+Mg_2FeH_6$ composite system, *International Journal of Hydrogen Energy*, 37 (2012) 6733-6740.
- [10] G.Q. Li, M. Matsuo, S. Deledda, R. Sato, B.C. Hauback, S. Orimo, Dehydrogenating Property of $LiBH_4$ Combined with Mg_2FeH_6 , *Mater. Trans.*, 54 (2013) 1532-1534.
- [11] BRUKER_AXS, TOPAS V4: General profile and structure analysis software for powder diffraction data, in, Karlsruhe, Germany, 2008.
- [12] M. Danaie, A.A.C. Asselli, J. Huot, G.A. Botton, Formation of the Ternary Complex Hydride Mg_2FeH_6 from Magnesium Hydride (β - MgH_2) and Iron: An Electron Microscopy and Energy-Loss Spectroscopy Study, *The Journal of Physical Chemistry C*, 116 (2012) 25701-25714.

Figure 1

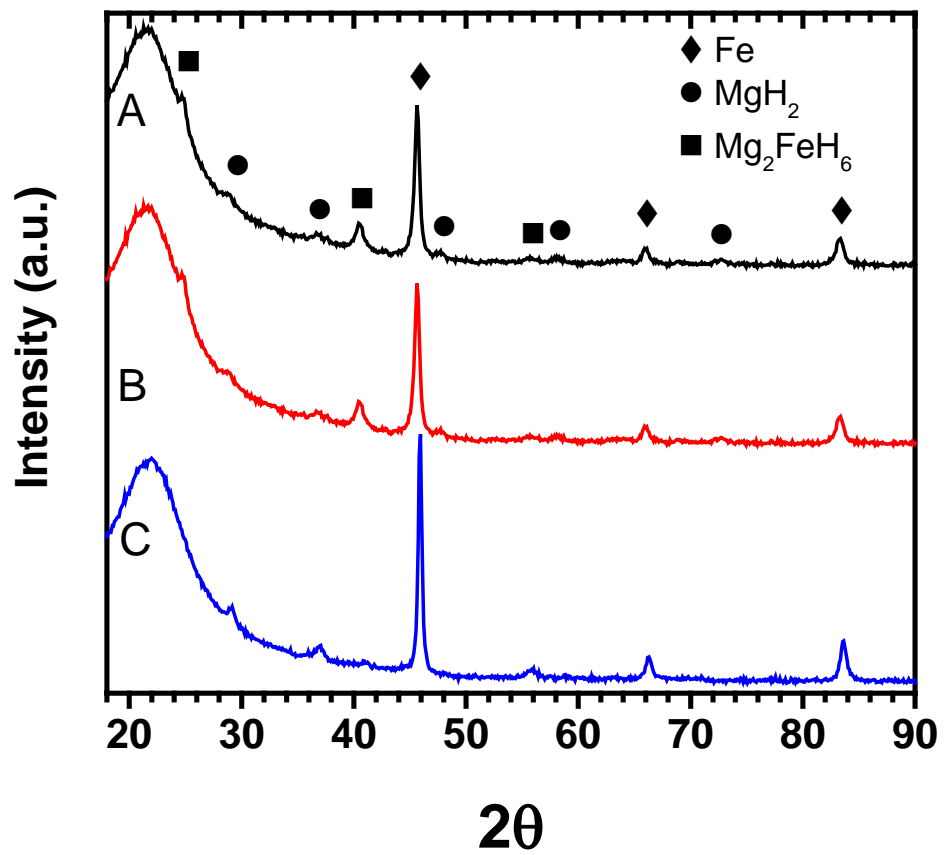


Figure 2

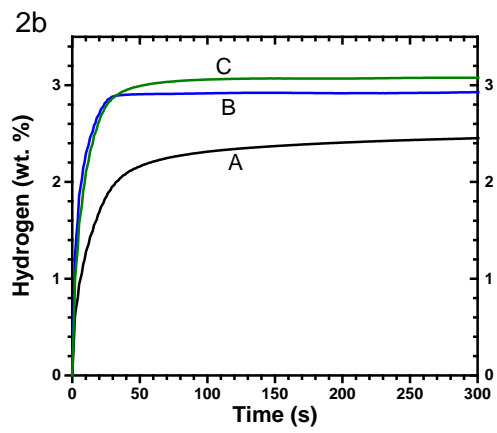
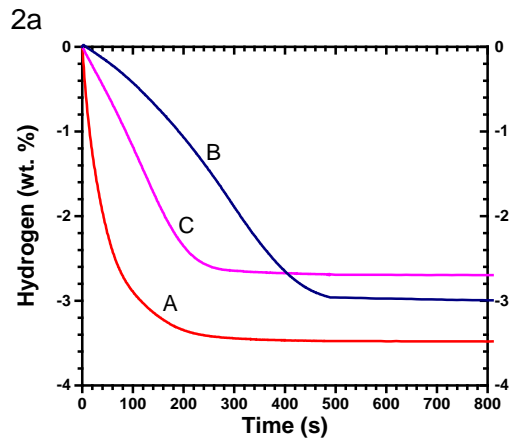


Figure 3

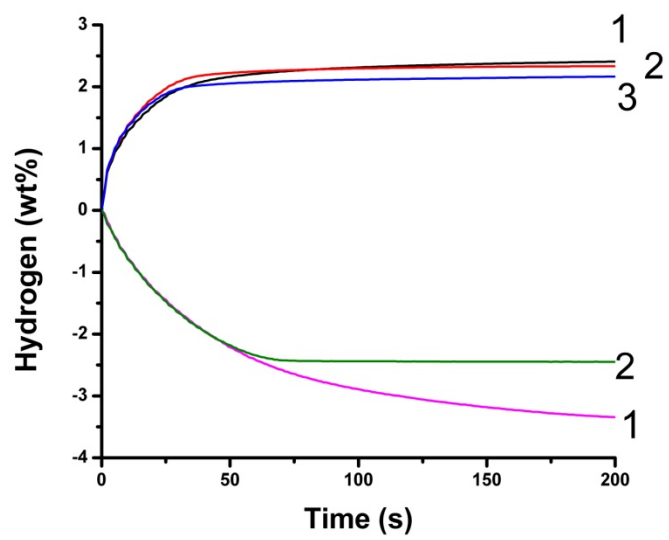


Figure 4

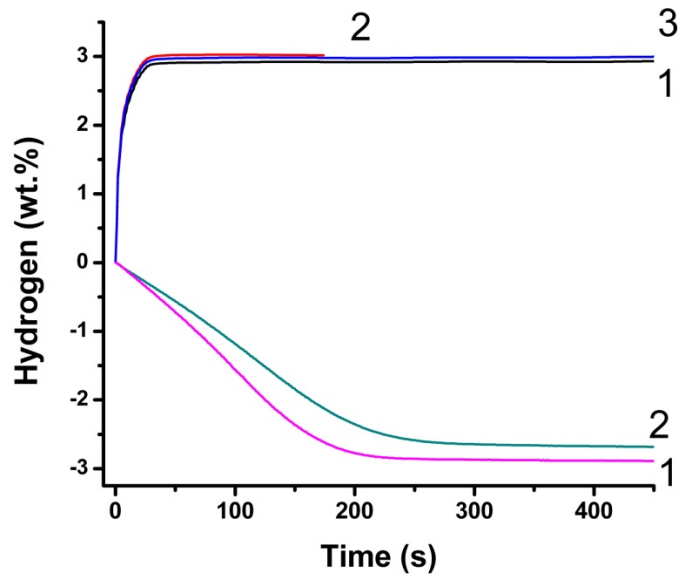


Figure 5

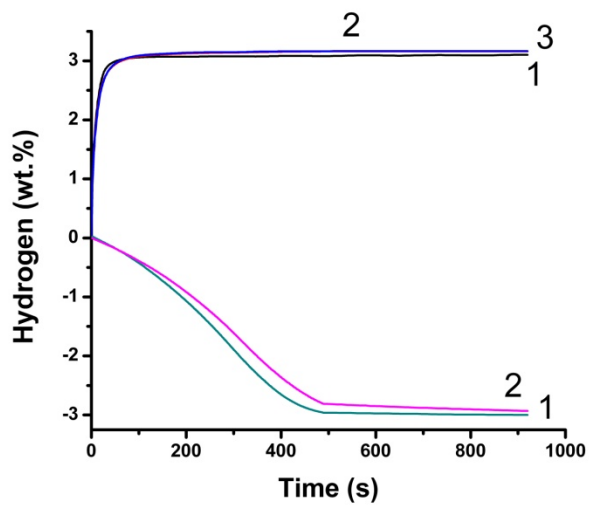


Figure 6

